JOURNAL OF PROPULSION AND POWER
Vol. 19, No. 5, September–October 2003

Atomic Emission Spectrometry for Profiling High Temperatures in Combustion System

Shigeo Yatsu*
Hokkaido University, Sapporo 060-8628, Japan
Hiroyuki Oyama†
National Institute of Advanced Industrial Science and Technology, Sapporo 062-8517, Japan
Takunari Mizuno‡
Hokkaido University, Sapporo 060-8628, Japan
Hideharu Kimura§
Matsushita System Engineering Co., Ltd., Sapporo 004-0015, Japan
Kuniyuki Kitagawa¶
Nagoya University, Nagoya 464-8603, Japan
and
Naoyuki Kayukawa**
Hokkaido University, Sapporo 060-8628, Japan

In this work a simple method was succesfully applied to observe profiles of high temperatures above 2000 K in a combustion field by combining a chemical seeding technique and a high-speed shuttering camera fitted with an optical bandpass filter. Spontaneous atomic emission profiles of chromium triplets from a partially premixed flame of acetylene-oxygen seeded with potassium chromate were measured to estimate the excitation temperature profile in the flame. An asymmetric Abel inversion was also successfully applied to illustrate radial profile of the excitation temperature. A significant difference in the profile was recognized between the results with and without this process. The lower temperature around the flame axis and a high-temperature donut in the middle zone were found and discussed in conjunction with mixing of acetylene and oxygen.

Nomenclature

A_{nm}	=	Einstein's transition probability for spontaneous emission, s^{-1}
$A_{1i,2i}$	=	transition probability from ith sublevel of chromium triplet 1, 2, 10^8 s^{-1}
c	=	velocity of light, ms^{-1}
E_j	=	energy of jth level, eV
E_n	=	term energy of upper level, eV
$E_{1i,2i}$	=	energy of ith sublevel of chromium triplet 1, 2, eV
g_j	=	statistical weight for jth level
g_n	=	statistical weight for upper level
$g_{1i,2i}$	=	statistical weight for ith sublevel of chromium triplet 1, 2
h	=	Planck's constant, Js
$I_{1,2}$	=	observed intensity of chromium triplet 1, 2, Wm^{-2}
$J_{1,2}$	=	spectral intensity of chromium triplet 1, 2, Wm^{-3}
k_B	=	Boltzmann's constant, $eVdeg^{-1}$
x	=	coordinate set along eyeline for observation, mm
y	=	coordinate set along longitudinal direction of flame, mm
z	=	coordinate set along transverse direction of flame, mm
ν_{nm}	=	frequency of spectral line for transition from nth level to mth one, s^{-1}
$\nu_{1i,2i}$	=	frequency of light from ith sublevel of chromium triplet 1, 2, s^{-1}
$\rho_{1,2}$	=	instrumental function for observation of chromium triplet 1, 2

Subscripts

i	=	sublevel of chromium triplet ($i = 1, 2, 3$)
j	=	energy level of atom
m	=	lower level of atomic energy state
n	=	upper level of atomic energy state
p	=	one of two triplets ($p = 1, 2$)

Received 9 September 2002; revision received 13 May 2003; accepted for publication 13 May 2003.

*Instructor, Center for Advanced Research of Energy Technology, Kita 13, Nishi 8, Kita-ku; sy@eng.hokudai.ac.jp.

†The New Energy and Industrial Technology Development Organization (NEDO) Fellow, Tsukisamu-Higashi, Toyohira-ku; currently Research Associate, Research Center for Advanced Energy Conversion, Nagoya University, Furo-cho, Chikusa-ku, Nagoya 464-8603, Japan.

‡Graduate Student, Center for Advanced Research of Energy Technology, Kita 13, Nishi 8, Kita-ku.

§System Engineer, Shimo-Nopporo Technopark, Atsubetsu-ku.

¶Professor, Research Center for Advanced Energy Conversion, Nagoya University, Furo-cho, Chikusa-ku. Member AIAA.

**Professor, Center for Advanced Research of Energy Technology, Kita 13, Nishi 8, Kita-ku. Member AIAA.

Introduction

In various fields, such as aeronautics, aerospace sciences, and energy conversion and furnace technologies, measurements of high temperatures above 2000 K in flames and combustion plasmas that are hardly measurable with conventional thermocouples are among the most important basic issues in conjunction with heat and mass balances, chemical composition, and thermodynamic characteristics during combustion. Conventional nonintrusive methods for temperature measurements include line-reversal method,[1] methods of spectral intensity ratio,[2–4] and laser techniques.[5] The line-reversal methods have widely been applied to combustion plasmas because their measurable temperature ranges are close to those of observed flames, intense resonance lines of seed elements lie in a visible region, and the instrumentation is relatively simple. However, most of conventional line-reversal methods are based on line-of-sight measurements and require laborious mapping to obtain temperature profiles. Thus, the spatial resolution is limited,

and the temperatures obtained are also dependent on the selected wavelength.

The two-wavelength planar laser-induced fluorescence technique[6] is among the most powerful tools for profiling of flame temperatures. Because the difference in energy between the levels is small for rotational levels of molecular species such as OH radicals, however, the precision would become poor at high temperature above 2000 K. In addition, sophisticated laser systems are not suitable for in situ field measurements under harsh conditions, such as industrial furnaces and propulsion engines.

Thus, simple and rugged methods are required for profiling of high flame temperatures above 2000 K. Recently, we have reported preliminary results obtained with a two-dimensional line-reversal method applied to a potassium-seeded acetylene-oxygen flame.[7] The details will be published elsewhere. In the previous studies our group developed a simple method for profiling high temperatures above 2000 K, by seeding an analyte flame with chromium and by using a high-speed digital camera fitted with an interference filter with a narrow optical bandpass width and applied to an C_2H_2/air flat flame.[8,9] In this study we applied this method to a C_2H_2/O_2 jet flame and also examined effects of the Abel inversion[10–12] to obtain the radial distribution of flame temperature.

Theoretical

The principle applied to our technique is based on the well-known two-line method,[13] or two-color method. In this study chromium was chosen as the seed element introduced in an acetylene/oxygen flame, and its two triplets of atomic emission were measured by a high-speed shuttering camera fitted with a narrow bandpass filter. The chromium triplets at the shorter and longer wavelengths are shown in Figs. 1 and 2, respectively, and the physical properties of their components are listed in Table 1 (Refs. 9, 14). These triplets are resulting from transitions with the relatively small excitation energies of about 3 eV and large transition probabilities to give easily detectable emission intensities at temperatures around 2000 K.

Table 1a Physical properties of the chromium triplets observed: triplet at shorter wavelength

Wavelength $c/\nu_{1i}(i=1,2,3)$, nm	Excitation energy $E_{1i}(i=1,2,3)$, eV	Weighted transition probability $g_{1i}A_{1i}$ $(i=1,2,3)$, 10^8/s
357.9	3.46	8.3
359.3	3.44	7.0
360.5	3.43	5.2

Table 1b Physical properties of the chromium triplets observed: triplet at longer wavelength

Wavelength $c/\nu_{2i}(i=1,2,3)$, nm	Excitation energy $E_{2i}(i=1,2,3)$, eV	Weighted transition probability $g_{2i}A_{2i}$ $(i=1,2,3)$, 10^8/s
425.4	2.91	2.0
427.5	2.90	1.5
429.0	2.89	0.95

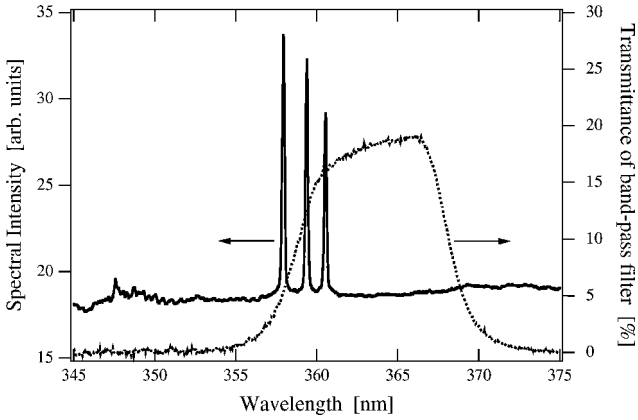

Fig. 1 Spectrum of the chromium triplet at the shorter wavelength (——) and transmittance of bandpass filter (· · · ·).

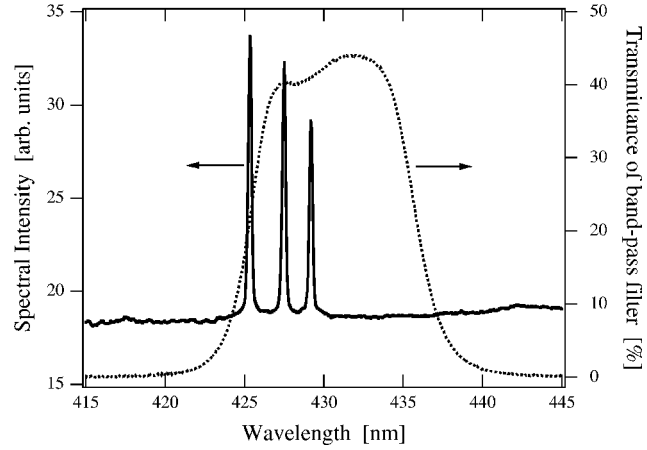

Fig. 2 Spectrum of the chromium triplet at the longer wavelength (——) and transmittance of bandpass filter (· · · ·).

However, the bandpass is not narrow enough to separate the triplet component lines. Thus, the intensity measured is the sum of the component intensities. The equations used to calculate the excitation temperature are given as follows.[9]

The spectral intensity of an atomic line is expressed by the following equations on the basis of the Boltzmann's distribution law:

$$J_{\mathrm{nm}} = h\nu_{\mathrm{nm}} A_{\mathrm{nm}} N_n \tag{1}$$

Here, the number density of the upper level N_n is given as a function dependent on the total number density of atoms of interest N and the excitation temperature T, namely,

$$N_n = [Ng_n/Q(T)]\exp(-E_n/k_BT) \tag{2}$$

where $Q(T)$ is the partition function expressed by the following equation:

$$Q(T) = \sum_j g_j \exp\left(\frac{-E_j}{k_BT}\right) \tag{3}$$

The spectral intensity of a chromium triplet is given by the following equation:

$$J_p = \left[\frac{hN}{Q(T)}\right]\sum_{i=1}^{3} \nu_{pi} g_{pi} A_{pi} \exp\left(\frac{-E_{pi}}{k_BT}\right) \qquad p = 1, 2 \tag{4}$$

The ratio of the two chromium triplets is expressed as follows:

$$\frac{J_1}{J_2} = \frac{\sum_{i=1}^{3} \nu_{1i} g_{1i} A_{1i} \exp(-E_{1i}/k_BT)}{\sum_{i=1}^{3} \nu_{2i} g_{2i} A_{2i} \exp(-E_{2i}/k_BT)} \tag{5}$$

Thus, the excitation temperature can be estimated from the intensity ratio of the two triplets. In practice, however, the intensity detected by the pixels of the camera detector is necessary to be corrected for the instrumental function depending on the wavelength, in conjunction with the transmittance of the optical components involved and the pixel sensitivity. In addition, the intensities observed by the camera pixels are those integrated through the flame thickness from x_0 to x_l along the eyeline, as given by the following equation:

$$I_p = \rho_p \int_{x_0}^{x_l} J_p(x)\,\mathrm{d}x \qquad p = 1, 2 \tag{6}$$

The Abel inversion is required to obtain the radial intensities of the chromium triplets. The algorithm used for this process in this study is an asymmetry version.[15]

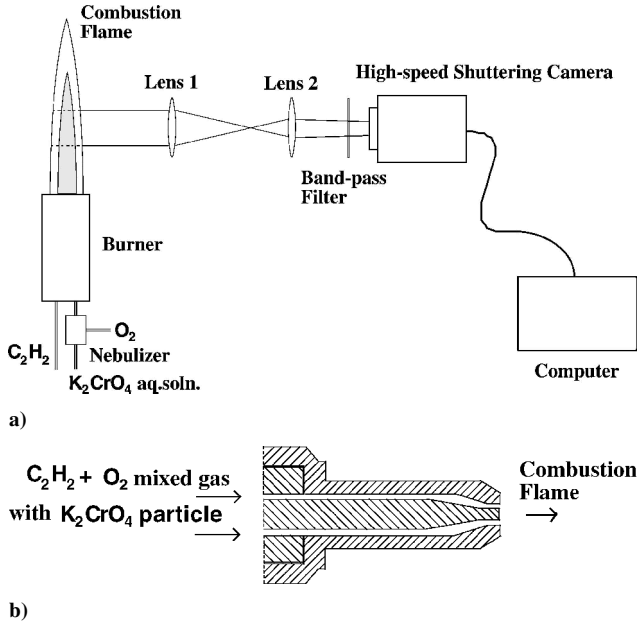

Fig. 3 Experimental system for measurement of flame temperature profile: a) top view of overall apparatus and b) cross section of burner nozzle.

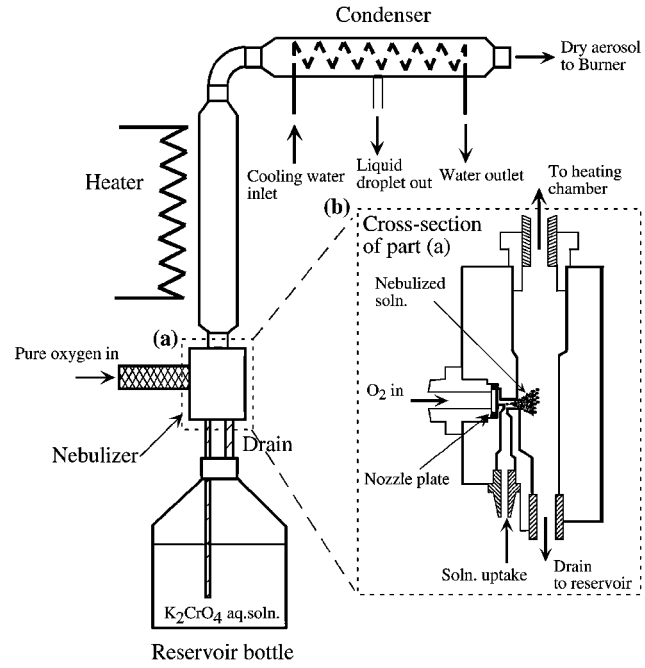

Fig. 4 Chromium-seeding apparatus.

Experimental

Instrumentation

Figure 3 shows the schematic diagram of the experimental system assembled for this study. The system consists of the premixed acetylene/oxygen flame supported on a conventional burner used for welding, the chromium seeding apparatus, the high-speed shuttering camera of a field size of 768×493 pixels, and an image intensifier with a variable gate width (shutter speed) ranging from 20 ns to 1 ms (Hamamatsu Photonics Model C4053) fitted with an optical bandpass filter, the dedicated interface, and the microcomputer (Macintosh Model 7100/80). The direction of burner axis is horizontal. A monochromatic flame image of spontaneous emission of chromium atoms is focused on the charge-coupled device (CCD) detector of the digital camera through the filter and the lens. Two filters with a transmittance of 20–45% and a bandpass width of 10 nm at 359 and 427 nm were used for the measurements of two chromium triplets, respectively (see Figs. 1 and 2). The gate width of the image intensifier was set at 1 μs. One-hundred twenty-eight frames were acquired at a rate of 30 frame/s and integrated on the interface memory to give a time-averaged image, followed by the computer storing and postprocessing.

Figure 4 shows the detail of the chromium seeding or introduction apparatus. This consists of the nebulizer (TSI Incorporated Model 3076), the heating chamber, and the condenser for desolvation. An aqueous solution of 5–10 gCr/ℓ as potassium chromate contained in the reservoir is taken up and nebulized with oxygen gas. The reagent of analytical grade and deionized water were used for the chromium solution. The particulates diameter ranges 0.02–0.3 μm (nominal) and the finer ones are transported into the heating chamber. The coarse particulates are drained back to the reservoir and recirculated for further nebulization. The aerosol water is vaporized in the heating chamber and drained out from the condenser. The resulting dry aerosols and the oxygen carrier gas are then mixed with the acetylene flow and fed to the burner (see Fig. 3b). The estimated amounts of chromium and potassium that reach the burner are 0.22–0.45 μg/min and 0.34–0.68 μg/min, respectively. The reduced flow rates of oxygen and acetylene were regulated at 3.43 and 1.95 ℓ/min with fluctuation within 2.5% throughout a run for 30 min, respectively. The flame generated by the burner is laminar steady jet flame.

The atomic emission spectra of the chromium triplets were observed by a multichannel spectrometer with a linear CCD detector of 1024 channels, a grating of 1200 grooves/mm, and a blaze wavelength of 500 nm (Hamamatsu Photonics Model C5095).

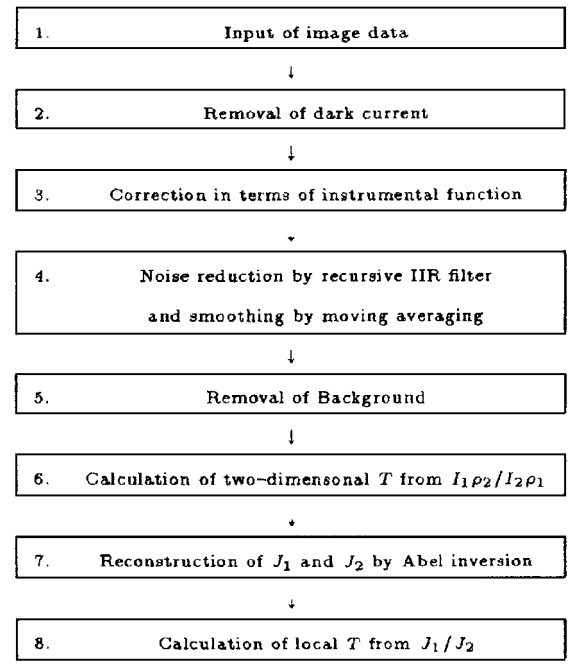

Fig. 5 Outline of image data processing.

Data Processing

Because background emission exists in the raw image data of the chromium triplet intensity, its removal is necessary to obtain the net spectral intensity. In addition, the correction is also necessary for the two chromium triplets with regard to the difference in the instrumental function depending on the wavelength. The data processing including these corrections is shown in Figure 5.

The background emission images for the chromium triplets $I_{1bg}(y, z)$ and $I_{2bg}(y, z)$ were separately measured with interference filters of central wavelengths 337 and 450 nm and a bandpass width of 10 nm, respectively. Here (y, z) is the coordinate of image. The pretreatment, or step 2, is applied to the four images thus obtained, the raw images $I_1(y, z)$ and $I_2(y, z)$ and the background images $I_{1bg}(y, z)$ and $I_{2bg}(y, z)$: the dark current images acquired before are subtracted from the raw image data pixel by pixel. The correction for the instrumental function, or step 3, includes the dependence

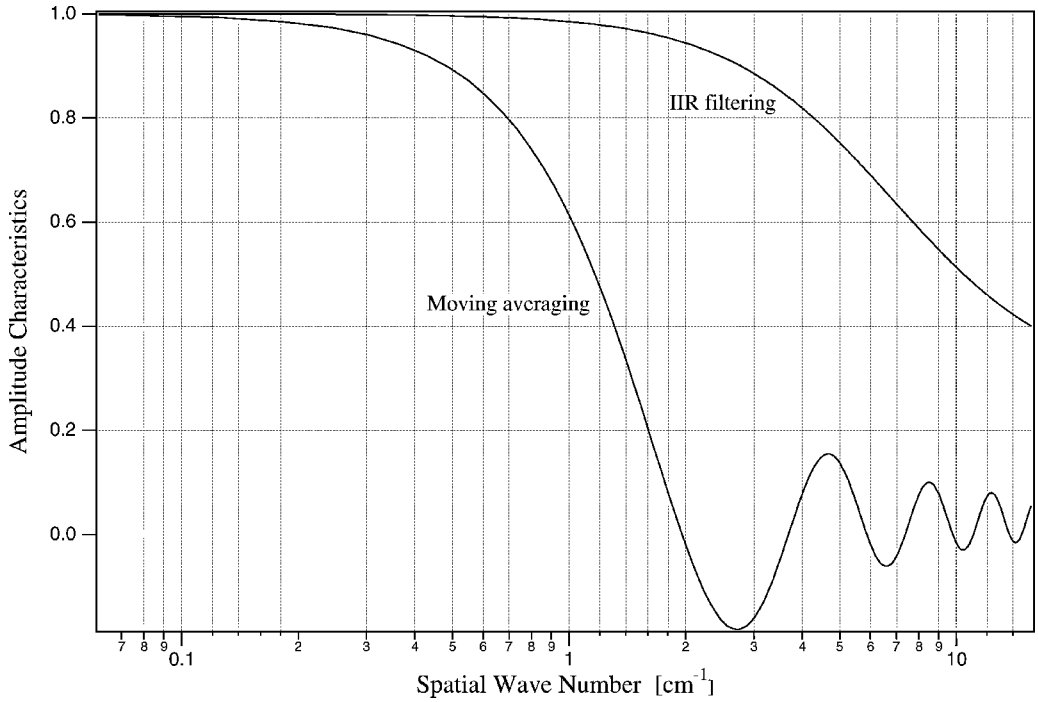

Fig. 6 Characteristics of the spatial filters.

of the image intensifier/CCD detector sensitivity on the wavelength, the CCD γ function, and the dependence of the transmittance of the optical elements. The overall wavelength dependence was calibrated using an National Institute of Standards and Technology Standard Lamp (Genaral Electric Company Model EPT-1336). Furthermore, detailed correction for likely spatial optical effects should be made. However, it was difficult because the effective area of the lamp filament was limited.

Step 4 involves operations of spatial averaging by a recursive infinite impulse response (IIR) filter[16] and a moving averaging[17,18] to remove high-frequency noises. Figure 6 shows the amplitude-wave-number characteristics of a low-frequency passing recursive IIR filter and a spatial moving-averaging filter used for numerical treatment in this step. In general, the spatial resolution is almost determined by the latter filter and is estimated to be about 6 mm based on the cutoff spatial frequency that is calculated from the curve in Fig. 6. Step 5 is for the background image correction.

Step 6 is the calculation of the excitation temperature image obtained by pixel-by-pixel calculations. The temperature profile is not a real radial distribution but more of averaged profile because the image intensity is observed as integrated along the transverse direction of the flame. Step 7 is the Abel inversion process to obtain the radial profiles of the spectral intensity. This process is applied to the image data after steps 1–5. The asymmetric Abel inversion is adopted to permit the process for both symmetric and cylindrically asymmetric emission profiles[19] along the flame axis. Finally, step 8 is the calculation of the radial profiles of excitation temperature.

Results and Discussion

Temperature Profile Without Abel Inversion

Figure 7 demonstrates the typical images of spontaneous emission intensities $I_1(y, z)$ and $I_2(y, z)$ of the chromium triplets at the a) shorter and b) longer wavelengths, obtained after the spatial averaging and background-subtraction processes (steps 1–5). The total time required for measuring a) the first image for 4.3 s, changing the optical filter and b) the second run was within 10 min. The left end of the image field corresponds to the position 73 mm downstream from the burner nozzle. The abscissa represents the longitudinal distance from the burner nozzle and the ordinate the transverse distance from the burner axis: the signs + and − indicate the upper and

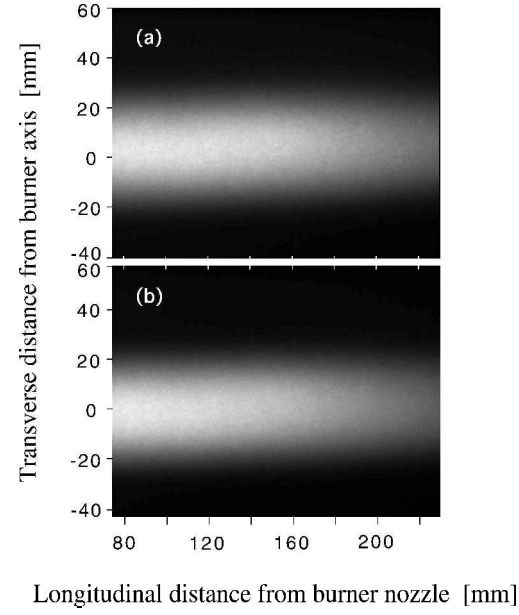

Fig. 7 Observed images of emission intensity for the triplets at the a) shorter and b) longer wavelengths.

lower direction from the horizontally supported flame, respectively. As seen from these figures, the combustion zone is within from −20 to +30 mm in the transverse direction. The flame length visually estimated was around 200 mm.

Figure 8 shows the temperature profile obtained by using Eq. (5) without the Abel inversion (step 6 in Fig. 5). The temperature in the central region of the flame is around 2250 K and becomes lower towards the peripheral zones: its gradient is steeper on the lower direction, compared with that on the upper one. This is probably caused by the buoyancy effect causing the flame asymmetry. The highest temperature exists in the central region above the burner nozzle or the upstream and becomes lower gradually along the longitudinal direction of the flame. The temperature measured with a line-reversal method of potassium, which is again not the radially resolved temperature, was 2200–2300 K in an area of 4 × 4 mm at

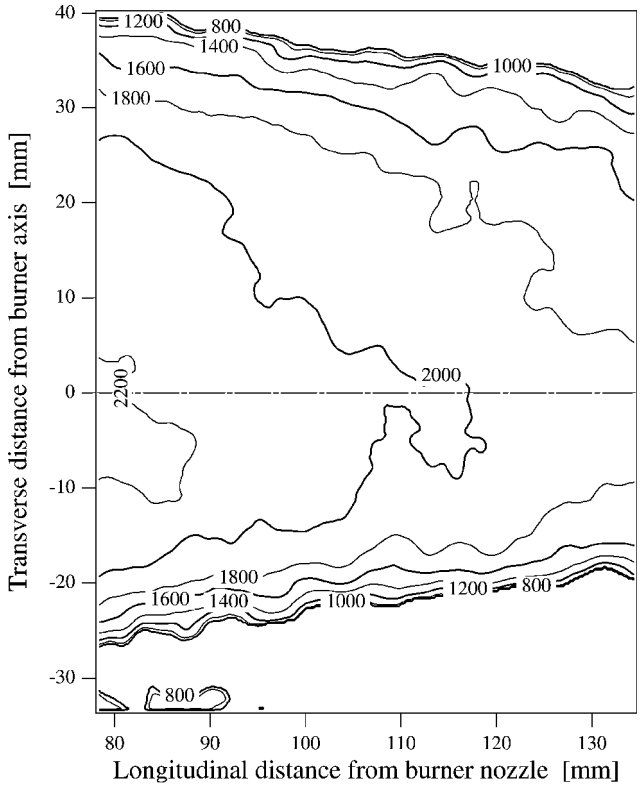

Fig. 8 Profile of excitation temperature without the asymmetric Abel inversion. Unit of numbers inside figure is Kelvin. Central line (– – – –) shows the elongation of burner axis.

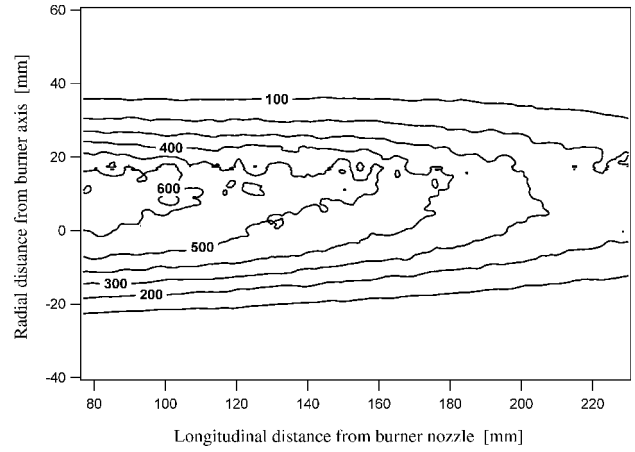

Fig. 9 Radial profiles of emission intensity for the triplet at the shorter wavelength after the asymmetric Abel inversion. Numbers inside figure shows relative intensity in an arbitrary unit.

the position 8.4 cm apart from the burner nozzle.[20,21] The temperature at the same position in Fig. 8 is around 2250 K and thus in good agreement within a relative error of 5%.

Radial Profiles of Atomic and Background Emission Intensities

The temperature profile shown in Fig. 8 does not reflect the real radial temperature profile because it is calculated with the intensity profiles integrated along the transverse direction of the flame. To obtain the radial temperature profile, the asymmetric Abel inversion was applied to the emission profiles (step 7 in Fig. 5). The results on the vertical cross section including the flame axis are shown in Figs. 9 and 10 for the triplets at the shorter and longer wavelengths, respectively. There are fluctuating contours of the emission intensity around the +17 mm off-axis region. This is mainly caused by the amplification of spatially high frequency caused by improper

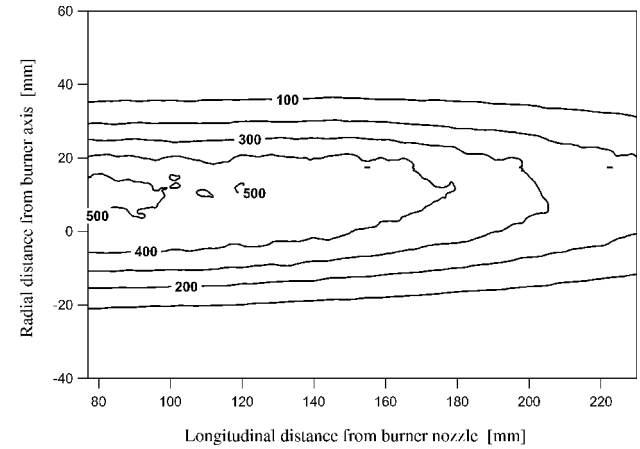

Fig. 10 Radial profiles of emission intensity for the triplet at the longer wavelength after the asymmetric Abel inversion. Numbers inside figure shows relative intensity in an arbitrary unit.

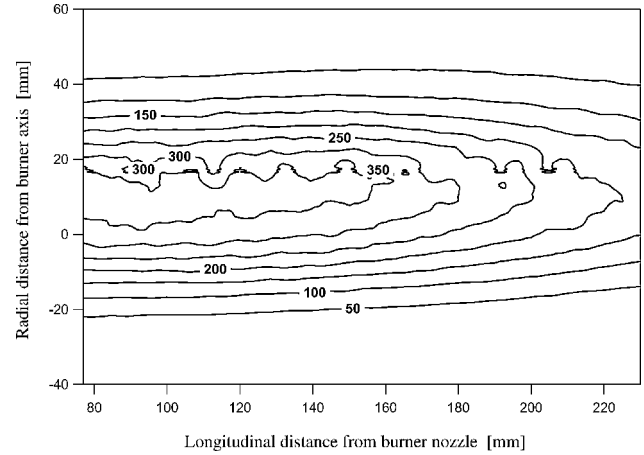

Fig. 11 Radial profile of the background emission near the chromium triplet at the longer wavelength after asymmetric Abel inversion. Numbers inside figure shows relative intensity in an arbitrary unit.

setting of the flame axis. In spite of uncertainty by such fluctuation, some characteristics of the flame can be recognized. In the longitudinal direction of the flame, the atomic emission intensity is higher around the flame axis for both of the chromium triplets. The spectral intensity of the triplet at the shorter wavelength becomes lower more significantly in the peripheral zones than that at the longer wavelength. This reflects that the excitation temperature is higher and lower in the central and peripheral regions, respectively. After the asymmetric Abel inversion the intensity is suppressed in the central region while it is enhanced in the peripheral ones (compare Fig. 7a with Fig. 9, and Fig. 7b with Fig. 10).

Figure 11 shows the radial profile of the background emission near the chromium triplet at the longer wavelength. The most likely species causing this background through the interference filter at 450 nm includes CH radicals with the band head wavelength of 431.2 nm. The background emission level was negligibly small near the chromium triplet at the shorter wavelength.

Radial Profile of Excitation Temperature

Figure 12 shows the typical radial profile of excitation temperature. A large difference in the temperature profile is recognized from a comparison of Figs. 8 and 12. In the radial profile there are two high-temperature regions in the middle zones, or three dimensionally a high-temperature donut, whereas without the Abel inversion the high-temperature region is given in the central region around the flame axis. Thus, the Abel inversion is effective to illustrate the real radial distribution. The temperature is lower by 200–300 K around the flame axis. This is mainly attributable to the incomplete

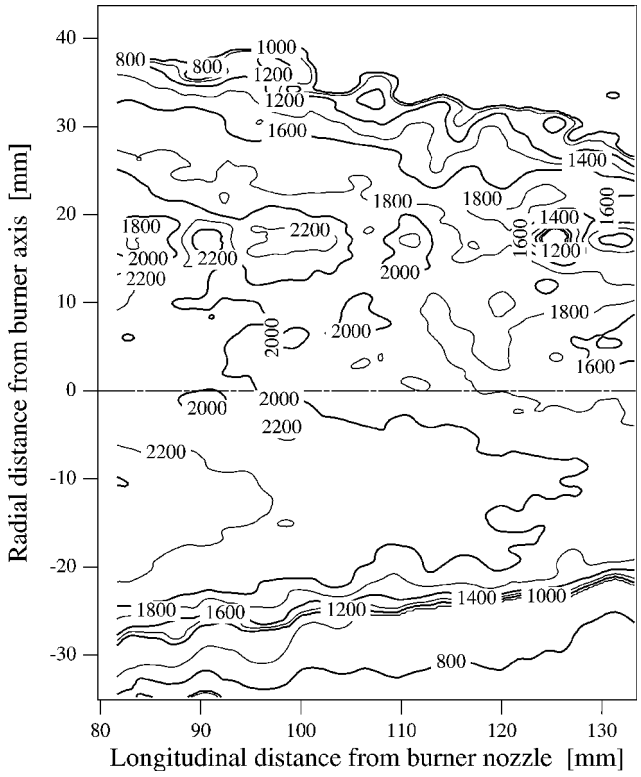

Fig. 12 Radial profile of the excitation temperature after asymmetric Abel inversion. Unit of numbers inside figure is Kelvin. Central line (– – – –) shows the elongation of burner axis.

combustion because of insufficient mixing of the fuel with oxygen supplied from the outer ring of the burner nozzle. In the donut region the oxygen is also supplied from the ambient air to allow more efficient combustion, and temperatures closer to adiabatic temperatures are attained consequently.

Conclusions

In this work a new temperature-profiling technique was developed by combining a two-line method of chromium triplets and the high-speed digital camera fitted with the optical interference filter. The excitation temperature was in good agreement with that obtained with the line-reversal method. To illustrate the radial distribution of the excitation temperature, the asymmetric Abel inversion was applied to the emission intensities of the chromium triplets, prior to the temperature calculation, and the results with and without this process were compared. The former profile indicated that the temperature was lower around the flame axis and that there was the high-temperature donut structure. This was reasonably explained by the difference in mixing rate in the radial location. There is a problem that is related to the precision in the asymmetric Abel inversion and reflects onto the radial profile of the excitation temperature. Another problem is that the seed element chromium is toxic for the environment. Iron is an alternative element usable for this method. The optimization of the flame-axis setting for the asymmetric Abel inversion and iron seeding are now under investigation.

Acknowledgments

The authors thank H. Niimi of Catalysis Research Center at Hokkaido University for his cooperation in our experiment. This work was sponsored partly by the Grant in Aid of the Ministry of Education, Science and Culture, Contact 08458113.

References

[1]Jeanmaire, P., "Application of Line Reversal Method to Measurement of Shock Flow Electron Temperature," *Physics of Fluids*, Vol. 17, No. 2, 1974, pp. 353–359.

[2]Griem, H. R., *Plasma Spectroscopy*, McGraw–Hill, New York, 1964, pp. 269–279.

[3]Huddlestone, R. H., and Leonard, S. L., *Plasma Diagnostic Techniques*, Series of Monographs and Textbooks, Vol. 21, Academic Press, New York, 1965, pp. 201–261.

[4]Griem, H. R., *Principles of Plasma Spectroscopy*, Cambridge Monographs on Plasma Physics, Vol. 2, Cambridge Univ. Press, Cambridge, England, U.K., 1997, pp. 279–289.

[5]Self, S. A., and Kruger, C. H., "Diagnostics Method in Combustion MHD Flows," *Journal of Energy*, Vol. 1, No. 1, 1977, pp. 25–43.

[6]Kirby, B. J., and Hanson, R. K., "Planar Laser-Induced Fluorescence Imaging of Carbon Monoxide Using Vibrational (Infrared) Transitions," *Applied Physics B (Lasers and Optics)*, Vol. B69, No. 5–6, 1999, pp. 505–507.

[7]Kayukawa, N., Kimura, H., Ito, Y., and Kitagawa, K., "On 2D Line Reversal Measurements with Monochromatic Imaging Spectroscopy," *Record of Workshop on New Energy and Environment*, FTE-00-22, The Institute of Electrical Engineers of Japan, Tokyo, Sept. 2000, pp. 1–6 (in Japanese).

[8]Bechtel, J. H., Blint, R. J., Dasch, C. J., and Weinberger, D. A., "Atomospheric Pressure Premixed Hydrocarbon-Air Flames: Theory and Experiment," *Combustion and Flame*, Vol. 42, No. 2, 1981, pp. 197–213.

[9]Kubota, M., Tsuge, S., Kitagawa, K., Arai, N., Ushigome, N., and Kato, Y., "Analysis of Degradation Processes of Carbon/Carbon Composition in a High Temperature Chemical Flame by a Spectrovideo Camera," *Carbon*, Vol. 36, No. 12, 1998, pp. 1783–1790.

[10]Barr, W. L., "Method for Computing the Radial Distribution of Emitters in a Cylindrical Source," *Journal of the Optical Society of America*, Vol. 52, No. 8, 1962, pp. 885–888.

[11]Griem, H. R., *Plasma Spectroscopy*, McGraw–Hill, New York, 1964, pp. 176–178.

[12]Blades, M. W., "Asymmetric Abel Inversions on Inductively Coupled Plasma Spatial Emission Profiles Collected from a Photodiode Array," *Applied Spectroscopy*, Vol. 37, No. 4, 1983, pp. 371–375.

[13]Haraguchi, H., Smith, B., Weeks, S., Johnson, D. J., and Winefordner, J. D., "Measurement of Small Volume Flame Temperature by the Two-Line Atomic Fluorescence Method," *Applied Spectroscopy*, Vol. 31, No. 2, 1977, pp. 156–163.

[14]Corliss, C. H., and Bozmann, C. H., "Experimental Transition Probabilities for Spectral Lines of Seventy Elements; Derived from the NBS Tables of Spectral-Line Intensities," U.S. Government Printing Office, Washington, DC, 1962, pp. 65–69.

[15]Yasutomo, Y., Miyata, K., Himeno, S., Enoto, T., and Ozawa, Y., "A New Numerical Method for Asymmetrical Abel Inversion," *IEEE Transactions on Plasma Science*, Vol. PS-9, No. 1, 1981, pp. 18–21.

[16]Press, W. H., Teukolsky, S. A., Vetterling, W. T., and Flannery, B. P., *Numerical Recipes in Fortran 77 Second Edition—The Art of Scientific Computing*, Cambridge Univ. Press, New York, 1992, pp. 530–602.

[17]Rosenfeld, A., and Avinash, C. K., *Digital Picture Processing*, Vol. 1, 2nd ed., Academic Press, Orlando, FL, 1982, pp. 250–264.

[18]Bracewell, R. N., *Two-Dimensional Imaging*, Prentice–Hall, Upper Saddle River, NJ, 1995, pp. 267–279.

[19]Oyama, H., Yatsu, S., Niimi, H., and Kayukawa, N., "Reconstruction of Potassium Atom Number Density in Flame from Observed Image Data," *Journal of the Japan Society of Applied Electromagnetics and Mechanics*, Vol. 8, No. 3, 2000, pp. 378–385 (in Japanese).

[20]Yatsu, S., Mizuno, T., Kitagawa, K., and Kayukawa, N., "Measurement of Acetylene-Oxygen Flame by Spectroscopic Image," *Proceedings for Symposium on Advanced Research of Energy Technology 2001*, Center for Advanced Research of Energy Technology, Hokkaido Univ., Sapporo, Japan, March 2001, pp. 111–114 (in Japanese).

[21]Mizuno, T., Yatsu, S., Kayukawa, N., and Kitagawa, K., "Investigation of Two Dimensional Temperature Distribution Measurement by Using Two-Colors Imaging Method," *Record of Workshop on New Energy and Environment*, FTE-01-39, The Institute of Electrical Engineers of Japan, Tokyo, Japan, Sept. 2001, pp. 61–66 (in Japanese).